

*Interpolymer complexes of Carbopol® 971
and poly(2-ethyl-2-oxazoline):
physicochemical studies of complexation
and formulations for oral drug delivery*

Article

Accepted Version

Creative Commons: Attribution-Noncommercial-No Derivative Works 4.0

Moustafine, R. I., Victorova, A. S. and Khutoryanskiy, V. V. (2019) Interpolymer complexes of Carbopol® 971 and poly(2-ethyl-2-oxazoline): physicochemical studies of complexation and formulations for oral drug delivery. *International Journal of Pharmaceutics*, 558. pp. 53-62. ISSN 0378-5173 doi: <https://doi.org/10.1016/j.ijpharm.2019.01.002> Available at <http://centaur.reading.ac.uk/81609/>

It is advisable to refer to the publisher's version if you intend to cite from the work. See [Guidance on citing](#).

To link to this article DOI: <http://dx.doi.org/10.1016/j.ijpharm.2019.01.002>

Publisher: Elsevier

All outputs in CentAUR are protected by Intellectual Property Rights law, including copyright law. Copyright and IPR is retained by the creators or other copyright holders. Terms and conditions for use of this material are defined in the [End User Agreement](#).

www.reading.ac.uk/centaur

CentAUR

Central Archive at the University of Reading

Reading's research outputs online

1 **Interpolymer complexes of Carbopol® 971 and poly(2-ethyl-2-oxazoline):**
2 **physicochemical studies of complexation and formulations for oral drug delivery**

3
4 Rouslan I. Moustafine,^{1*} Anastasiya S. Viktorova,¹ Vitaliy V. Khutoryanskiy^{1,2*}

5
6 ¹ Institute of Pharmacy, Kazan State Medical University, 16 Fatykh Amirkhan Street, 420126
7 Kazan, Russian Federation

8 ² Reading School of Pharmacy, University of Reading, Whiteknights, PO box 224, Reading
9 RG66AD, United Kingdom

10
11 **Abstract**

12 Carbopol® 971 and poly(2-ethyl-2-oxazoline) form hydrogen-bonded interpolymer complexes
13 in aqueous solutions and their complexation is strongly dependent on solution pH. This work
14 investigated the complexation between these polymers in aqueous solutions. The compositions
15 of interpolymer complexes as well as the critical pH values of complexation were determined.
16 The structure of these complexes was studied in solutions using transmission electron
17 microscopy and in solid state using elemental analysis, FTIR spectroscopy and differential
18 scanning calorimetry. Solid compacts were prepared based on interpolymer complexes and
19 physical blends of these polymers and their swelling behaviour was studied in aqueous
20 solutions mimicking the fluids present in the gastrointestinal tract. These materials were used
21 to prepare oral formulations of mesalazine and its release from solid matrices was studied in
22 vitro. It was demonstrated that the complexation between Carbopol® 971 and poly(2-ethyl-2-
23 oxazoline) has a profound effect on the drug release from matrix tablets.

24
25 **Keywords:** interpolymer complexes, Carbopol®, polyoxazoline, hydrogen bonding,
26 nanoparticles, critical pH, mesalazine, oral drug delivery

27
28 *Correspondence: Dr Rouslan I. Moustafine rouslan.moustafine@gmail.com and Prof Vitaliy
29 V. Khutoryanskiy v.khutoryanskiy@reading.ac.uk

30 **1. Introduction**

31 Hydrophilic polymers and their combinations are often used to formulate dosage forms as they
32 provide a number of unique features required for successful drug delivery. When polymer
33 combinations are used for this purpose the performance of the resulting material is often
34 affected by specific attractive interactions occurring between them. The most common types
35 of specific interactions are electrostatic attraction and hydrogen bonding. Electrostatic
36 attraction may occur in combinations of oppositely charged polyelectrolytes and typically
37 results in formation of interpolyelectrolyte complexes (Mustafin, 2011). Hydrogen-bonded
38 interpolymer complexes (IPC) are commonly formed as a result of interactions between
39 polycarboxylic acids, acting as proton donors, and non-ionic water-soluble polymers,
40 exhibiting proton-accepting properties (Bekturov and Bimendina, 1981; Kemenova et al, 1991;
41 Khutoryanskiy, 2007; Kharlampieva et al, 2009).

42 Poly(2-oxazolines) is an interesting class of functional materials, which is represented by
43 several polymers soluble in water (e.g. poly(2-methyl-2-oxazoline), poly(2-ethyl-2-oxazoline),
44 poly(n-propyl-2-oxazoline, etc). The synthesis of these polymers was first described in the
45 1960s; however, they received recognition as highly promising biomedical materials only in
46 the last decade (Hoogenboom, 2009; Viegas et al, 2011; Luxenhofer et al, 2012; de la Rosa,
47 2014; Hoogenboom and Schlaad, 2017; Lorson et al, 2018). Numerous recent studies reported
48 the use of poly(2-oxazolines) in the design of micellar structures for drug delivery (Hruby et
49 al, 2010), vectors for gene therapy (Lehner et al, 2017), hydrogels (Farrugia et al, 2013),
50 polymer-drug/protein conjugates (Mero et al, 2008), and mucus-penetrating nanoparticles
51 (Mansfield et al, 2015; Mansfield et al, 2016). Polyoxazolines are generally non-toxic,
52 biocompatible, and bioinert, which makes them highly promising for various biomedical
53 applications. These polymers are often viewed as an alternative to polyethylene glycols
54 (Bludau et al 2017; Khutoryanskiy, 2018).

55 Water-soluble poly(2-oxazolines) exhibit a number of interesting physicochemical properties
56 such as temperature-responsive behaviour (Christova et al, 2003; Diehl and Schlaad, 2009;
57 Ambreen and Siddiq, 2014) and proton-accepting ability that facilitates their interactions with
58 proton-donating polymers (Kim et al, 2002). These properties have been successfully utilised
59 in the development of self-assembled materials such as micelles (Filippov et al, 2017),
60 interpolymer complexes and polymeric blends (Dai et al, 1994; Isasi et al, 1996; Kim et al,
61 2002), and multi-layered constructs (Su et al, 2017; Su et al, 2018).

62 The application of poly(2-oxazolines) in the design of solid dosage forms for drug delivery has
63 also received recent interest, but it is still studied insufficiently (Claeys et al, 2012; Policianova
64 et al, 2014; Fael et al, 2018). Recently, interpolymer complexes and physical blends of poly(2-
65 ethyl-2-oxazoline)s and two Carbopol[®] grades (Carbopol[®] 974 and Carbopol[®] 971) were
66 reported for the development of mucoadhesive tablets for buccal delivery of hydrocortisone
67 (Ruiz-Rubio et al, 2018). It was demonstrated that the interaction between these polymers is
68 pH-dependent and the behaviour of tablets is strongly affected by the interactions between the
69 polymers. Taking the pH-responsive nature of these complexes they could also be of interest
70 as materials for oral drug delivery, where a dosage form will experience different pH
71 environments during its transit through gastrointestinal tract.

72 In the present study the complexation between Carbopol[®] 971 and poly(2-ethyl-2-oxazoline)
73 of different molecular weights was explored both in solutions and in solid state. The effect of
74 solution pH on the complexation between polymers was explored and the critical pHs of
75 complexation were determined. The structure of interpolymer complexes in solid state was
76 studied by elemental analysis, FTIR spectroscopy and differential scanning calorimetry. Solid
77 compacts composed of either IPCs or physical mixtures (PMs) were studied in the media
78 mimicking different parts of gastrointestinal tract. These solid materials were used to formulate
79 a model drug mesalazine relevant for gastrointestinal drug delivery and its release from the
80 dosage forms was studied in vitro.

81

82 **2. Materials and Methods**

83 **2.1. Materials**

84 Poly(2-ethyl-oxazoline)s (5000, 50000, 500000 g mol⁻¹; named as POZ 5 kDa, POZ 50 kDa
85 and POZ 500 kDa in the text, respectively) were purchased from Sigma-Aldrich (Irvine, UK)
86 and Carbopol[®] 971 (weakly cross-linked, 4000-11000 cP, 3000 kDa) (named as C971 in the
87 text), was generously donated by Lubrizol Advanced Materials (Wickliffe, OH, U.S.A.).
88 Potassium dihydrogen phosphate, hydrochloric acid and sodium hydroxide were provided by
89 Sigma-Aldrich (Irvine, UK) and used for preparing the media mimicking conditions of gastro-
90 intestinal tract. Mesalazine (5-aminosalicylic acid, 5-ASA) was purchased from Sigma-Aldrich
91 (Irvine, UK). A Milli-Q water purification system from Millipore (Bedford, MA, U.S.A.) was
92 used for preparation of all solutions.

93

94 **2.2. Methods**

95 *2.2.1 IPC formation*

96 Aqueous mixtures were prepared by mixing 0.002 unit-mol/L individual polymer solutions in
97 deionized water. Solutions were mixed to give different unit molar ratios of the polymer
98 components. The obtained interpolymer complexes (IPCs) were left for 1 hour in the media,
99 and then turbidity of all solutions was measured spectrophotometrically (Lambda 25, Perkin
100 Elmer, Norwalk, CT, U.S.A.) at 400 nm. The complexation between C971 and POZ was
101 initially evaluated in water without adjusting the pH.

102

103 For pH_{crit} determination, samples were typically analyzed in solutions, whose pH
104 ranged from 3.0 to 8.0, which was adjusted by adding small portions of 0.1 M NaOH or 0.1 M
105 HCl. The pH measurements were performed using a portable pH meter Orion Star A 325
106 (Thermo Scientific, U.S.A.) with Orion™ ROSS Ultra™ low maintenance pH/ATC Triode™
107 (Thermo Scientific, U.S.A.). The turbidity of these solutions was measured at 400 nm using a
108 UV/Vis-spectrophotometer (Lambda 25, Perkin Elmer, Norwalk, CT, U.S.A.). Turbidity
109 readings were taken immediately after adjusting pH. All experiments were repeated in
110 triplicate, and the turbidity values are reported as mean \pm standard deviation.

111

112 The composition with the maximal turbidity was selected for the tablet formulation. IPCs were
113 prepared by mixing 0.1 M POZ and 0.125 M C971 solutions in acetate buffer (pH=3.5) and at
114 constant temperature. After isolation of the precipitates from the solutions, they were washed
115 twice with demineralized water and the IPCs were subsequently freeze-dried for 2 days at -27
116 °C (Labconco® Freeze Dry System, FreeZone 1 L, MO, U.S.A.). The dried IPCs were ground
117 with A 11 basic grinder (IKA® Werke GmbH, Staufen, Germany) and used for further study.
118 The samples were stored in tightly sealed containers at room temperature.

119

120 *2.2.2. Transmission electron microscopy (TEM)*

121 TEM images of IPC were acquired using a JEM 2100 plus TEM (Jeol Ltd., Watchmead
122 England) at 200 kV. For sample preparation, the copper grids were brought in contact with
123 dispersions of IPC for 30 s and then dried off with a filter paper. The pH of polymer mixtures
124 in aqueous solutions prior to TEM examination was adjusted by adding small amounts of 0.2
125 mol/L HCl or NaOH and was measured using a digital pH-meter (Metrohm, Herisau,
126 Switzerland).

127

128 *2.2.3. Elemental analysis*

129 The composition of freeze-dried IPC (C971/POZ 50 kDa and C971/POZ 500 kDa) samples
130 and physical mixture (PM) samples before, during, and after swelling testing were investigated
131 by elemental analysis using a Thermo Flash 2000 CHNS/O elemental analyzer (Thermo Fisher
132 Scientific, Paisley, UK). PMs were prepared by mixing C971 and POZ powders at 1.25:1 molar
133 ratio.

134

135 *2.2.4. Fourier transform infrared spectroscopy (ATR-FTIR)*

136 ATR-FTIR-spectra were recorded using a Nicolet iS5 FTIR spectrometer (Thermo Scientific,
137 Waltham, MA, U.S.A.). The untreated freeze-dried samples of solid IPC (C971/POZ 50 kDa
138 and C971/POZ 500 kDa) and PM samples before, during, and after swelling testing were
139 directly mounted over the iD5 smart single bounce ZnSe ATR crystal. The spectra were
140 analyzed using OMNIC spectra software.

141

142 *2.2.5. Thermal analysis*

143 Modulated DSC (mDSC) measurements were carried out using a Discovery DSC™ (TA
144 Instruments, New Castle, DE, U.S.A.), equipped with a refrigerated cooling system (RCS90).
145 TRIOSTM software (version 3.1.5.3696) was used to analyze the results (TA Instruments, New
146 Castle, DE, U.S.A.). Tzero aluminum pans (TA Instruments, New Castle, DE, U.S.A.) were
147 used in all calorimetric studies. The empty pan was used as a reference and the mass of the
148 reference pan and of the sample pans were taken into account. Dry nitrogen at 50 mL/min was
149 used as a purge gas through the DSC cell. Indium and n-octadecane standards were used to
150 calibrate the DSC temperature scale; enthalpic response was calibrated with indium. The
151 modulation parameters used were: 2 °C/min heating rate, 40 s period and 1 °C amplitude.
152 Calibration of heat capacity was done using sapphire. Samples were analyzed from 0 to 200
153 °C.

154

155 *2.2.6. Preparation of Tablets*

156 To determine the degree of swelling, flat-faced tablets of 100 mg polymer carrier were prepared
157 by compressing the given amount of powders (C971, POZ 50 kDa, POZ 500 kDa, PMs, and
158 IPCs) in a hydraulic press (Perkin Elmer, Waltham, MA, U.S.A.), equipped with flat-faced
159 punches with 13 mm diameter (Pike Technologies, Madison, WI, U.S.A.) with a compression
160 pressure of 6.24 MPa. For dissolution testing, 150 mg biconvex tablets (100 mg 5-ASA and 50

161 mg polymer carrier) with 6 mm diameter were prepared by compressing the given amount of
162 the polymer carriers at 6.24 MPa using a hydraulic press (Perkin Elmer, Waltham, MA,
163 U.S.A.).

164

165 *2.2.7. Determination of the Degree of Swelling of Matrices*

166 Swelling was investigated under conditions, mimicking the gastro-intestinal tract (GIT): the
167 first two hours in simulated gastric medium (0.1 M HCl; pH 1.2), then four hours in simulated
168 intestinal medium (phosphate buffer; pH 6.8).

169

170 *2.2.7.1. Gravimetric measurements*

171 The polymer matrices (d=13 mm) were placed in a tarred basket (from USP I apparatus), which
172 was immersed into a thermostatted bath at 37.0 ± 0.5 °C on IC control eco 18c (IKA® Werke
173 GmbH, Staufen, Germany). The volume of the medium was 100 mL. The basket was removed
174 from the medium every 15 min within the first hour and then every 30 min; the tablets were
175 carefully dried using a filter paper and weighed. The degree of swelling (H, %) was calculated
176 using the following equation:

177

$$H\% = (m_2 - m_1 / m_1) \times 100,$$

178 where m_1 is the weight of the dry sample and m_2 is the weight of the swollen sample.

179

180 *2.2.7.2. Image analysis*

181 The polymer matrices (d=13 mm) were placed into petri dishes with 40 mL of the medium
182 preheated to 37.0 ± 0.5 °C. The petri dishes with matrices were removed from thermostatted
183 bath every 1 hour, placed on a graph paper and changes in the sizes of the matrices were
184 measured.

185

186 *2.2.8. Release of mesalazine (5-ASA) from the polymer matrices in GIT mimicking conditions*

187 The release of 5-ASA from the matrix tablets was performed under sink conditions at $37.0 \pm$
188 0.1 °C using the USP I Apparatus (the off-line dissolution tester DT 828 with an auto sampler
189 ASS-8, a fraction collector FRL 824 and a peristaltic pump ICP-8 (Erweka, Heusenstamm,
190 Germany)). The basket rotation speed was 100 rpm and the volume of the medium was 900
191 mL. The release was investigated for 6 h under GIT mimicking conditions, where the pH of
192 the release medium was gradually increased: 2 h in 0.1 M hydrochloric acid (pH = 1.2) and
193 then in phosphate buffer solution (pH = 6.8) until the end of experiment. Aliquots (5 mL) of
194 solution were automatically taken at specific time intervals, and the volume of medium was

195 made up to the original value by adding fresh dissolution medium. The amounts of 5-ASA
196 released in the dissolution medium were determined by UV/Vis-spectrophotometry at 302 nm
197 (at pH=1.2) and 330 nm (at pH=6.8), respectively (Lambda 25; Perkin-Elmer, Waltham, MA,
198 U.S.A.). Results are given as the mean values of three determinations \pm standard deviations.
199 Release rates (RR) were determined by calculating the slopes of the released 5-ASA (%) vs
200 time profiles in the first 120 min of experiment.

201

202 **Results and Discussion**

203 *3. Formation of interpolymer complexes in aqueous solutions*

204 Simple mixing of 0.002 unit-mol/L aqueous solutions of C971 and POZ (without adjustment
205 of pH) at room temperature results in immediate appearance of turbidity, which was used to
206 estimate the compositions of IPCs formed. **Figure 1** presents the turbidity data for the polymers
207 mixed at different molar ratios. It is widely recognised that the maximal values of turbidity
208 generally correspond to the compositions of IPC (Sato et al, 1989; Takayama et al, 1990;
209 Moustafine et al, 2006). POZ 50 kDa exhibited greater ability to increase the turbidity of
210 solution mixtures with the maximal values observed at [C971]:[POZ]=1.25:1 mol/mol. Similar
211 trend is observed for POZ 500 kDa; however, its turbidity is significantly lower ($p < 0.005$).
212 POZ 5 kDa exhibited much lower ability to increase the solution turbidity in mixtures with
213 C971.

214 **(Figure 1 is here).**

215 It could be anticipated that these polymers should form 1:1 complexes, i.e. one unionised
216 carboxylic group of C971 forms hydrogen bond with one proton-accepting nitrogen according
217 to the proposed scheme (**Figure 2**). A deviation from 1:1 ratio observed in our experiments
218 could be related to two factors: (1) a weakly cross-linked nature of C971, which results in steric
219 hindrances and not complete availability of carboxylic groups of polyacid to interact with POZ;
220 (2) under the pH conditions of this experiment not all carboxylic groups of C971 are non-
221 ionised and capable of forming hydrogen bonds with POZ. This result agrees with the previous
222 studies of C971 – POZ complexes using gravimetric analysis (Ruiz-Rubio et al, 2018).

223 **(Figure 2 is here)**

224 Previously, Khutoryanskiy and co-workers (Mun et al, 2000; Nurkeeva et al, 2003;
225 Khutoryanskiy et al, 2004a; Khutoryanskiy et al, 2004b; Nurkeeva et al, 2005; Zhunuspayev

226 et al, 2008) have demonstrated that the complexation between poly(carboxylic acids) and non-
227 ionic polymers is facilitated under acidic conditions and formation of colloidal IPCs is typically
228 observed below a certain critical pH of complexation (pH_{crit}). pH_{crit} values were proposed as a
229 criterion for the ability of a given pair of polymers to form hydrogen-bonded IPCs: greater
230 pH_{crit} indicated a stronger ability of polymers to form complexes. To the best of our knowledge,
231 the data on pH_{crit} of complexation involving poly(2-oxazolines) is still very limited in the
232 literature. Su et al (2017) recently reported that the thickness of multilayered films, formed
233 using layer-by-layer deposition of poly(acrylic acid) (PAA) and POZ onto a solid substrate,
234 showed a pH dependence, typical for hydrogen-bonded IPCs: a rapid increase in the film
235 thickness is observed upon decrease in pH in the 3.5-4.0; above pH 4.0 the films did not form.
236 The authors assigned the pH 3.5-4.0 to the critical pH of complexation between these polymers.
237 In the present work the critical pHs were determined for Carbopol[®] 971 – POZ complexes
238 using turbidimetric technique. **Figure 3** shows the dependence of solution turbidity of 1:1
239 polymer mixtures as a function of pH. It is clearly seen that a decrease in solution pH results
240 in a rapid increase in turbidity at $pH\ 4.8\pm 0.2$, when POZ 50 kDa was used to form IPC. This is
241 slightly larger than the pH_{crit} reported by Su et al (2017) for complexes of POZ 50 kDa with
242 PAA, but the discrepancy may be related to the difference in the methods used to determine
243 pH_{crit} (film formation vs turbidimetric studies) and also the weakly cross-linked nature of
244 Carbopol[®] 971 compared to PAA.

245 **(Figure 3 is here)**

246 POZ with lower (5 kDa) and larger (500 kDa) molecular weights show their pH_{crit} around 4.2-
247 4.5 (no significant difference between pH_{crit} for 5 kDa and 500 kDa ($p>0.05$), but significantly
248 lower than pH_{crit} for 50 kDa ($p<0.05$)). It is well known from the literature (Mun et al, 2000;
249 Nurkeeva et al, 2003; Khutoryanskiy et al, 2004a; Khutoryanskiy et al, 2004b; Nurkeeva et al,
250 2005) that increase in molecular weight of the polymers typically leads to increase in pH_{crit} . An
251 anomalous lower complexation ability of POZ 500 kDa observed in experiments presented in
252 Figure 1 (lower turbidity values) and also lower pH_{crit} values compared to POZ 50 kDa (Figure
253 2) is possibly related to extremely large length of POZ 500 kDa macromolecules that approach
254 so-called upper limit in molecular weights of polymers, previously reported by Bekturov and
255 Bimendina (1981).

256 A comparison of pH_{crit} values, previously reported for complexes of PAA and poly(N-vinyl
257 pyrrolidone) $pH_{crit}=4.85\pm 0.05$, poly(methyl vinyl ether) $pH_{crit}=4.85\pm 0.05$, polyacrylamide

258 $pH_{crit}=3.00 \pm 0.05$, poly(ethylene oxide) $pH_{crit}=2.88 \pm 0.05$, poly(vinyl alcohol) $pH_{crit}=2.67 \pm$
259 0.05 and some other polymers (Khutoryanskiy et al, 2004a), with the values determined for
260 POZ in the present work allows to conclude that poly(2-ethyl-2-oxazoline) exhibits strong
261 complexation ability. This ability to form IPCs is comparable with poly(N-vinyl pyrrolidone)
262 and poly(methyl vinyl ether). It should be noted that in the current study we used polymer
263 concentrations of 0.01 unit-mol/L similar to the measurements reported by Khutoryanskiy et
264 al (2004a); however, the difference in the two studies is in the use of Carbopol[®] 971 (weakly
265 cross-linked PAA, 3000 kDa) and linear PAA 450 kDa.

266 In order to get an insight into the changes in the structure of IPCs at different pHs
267 transmission electron microscopy (TEM) was used (**Figure 4a**). This experiment provides an
268 excellent opportunity to see the evolution of IPC structure upon gradual decrease in solution
269 pH. At pH 4.79, which is very close to pH_{crit} the structure of IPC looks like a network of fibrous
270 material with the presence of some very small particles (18 ± 6 nm). Upon decrease in pH to
271 4.54 these particles become larger and denser (41 ± 4 nm), but still are surrounded and connected
272 to each other by fibrous material, which is possibly made of not fully complexed
273 macromolecules. Under strongly acidic conditions the dense particles of IPC are fully formed;
274 they are not stabilised by uncomplexed macromolecules and their size reaches 649 ± 185 nm
275 (pH 2.14) and 513 ± 92 nm (pH 2.50). Very similar structural changes at different pHs were
276 reported previously for the IPC formed by PAA and methylcellulose (Khutoryanskaya et al,
277 2007). The proposed mechanism of IPC formation at different pHs is shown in **Figure 4b**.

278 (**Figure 4 is here**)

279 *4. Physicochemical studies in solid state*

280 *4.1. Fourier transform infrared spectroscopy (ATR-FTIR)*

281 ATR-FTIR spectrum of pure POZ independently from its molecular weight is characterized
282 by the presence of a stretching band of amide I at 1635 cm^{-1} . For C971, the band corresponding
283 to the self-associated carboxylic group (COOH) is located at 1703 cm^{-1} (Nguyen et al., 2016;
284 Ruiz-Rubio et al., 2018; Garipova et al, 2018). Clearly, the presence of POZ and C971 in the
285 spectrum of the polymer mixture (PM) is indicated by their characteristic peaks with high
286 intensities, such as the peak of the carboxyl stretching band of C971 (1705 cm^{-1}) and a
287 “shoulder” of amide I of POZ (1635 cm^{-1}). In the IPC, a shift of the C=O bands could be
288 observed to 1720 cm^{-1} , while the amide I band shifts to 1600 cm^{-1} . These bands are related to
289 hydrogen bond formation between carboxyl groups of C971 and amide groups of POZ.

290 **(Figure 5 is here)**

291 4.2. Thermal analysis

292 **Figure 6(a, b)** shows the DSC thermograms of C974, POZ 50 kDa (a), POZ 500 kDa (b),
293 their PMs and IPCs. Carbopol 974 presents a T_g at 132.6 °C, whereas the T_g of POZ 50 and
294 POZ 500 kDa are detected at 51.7 and 56.2°C, respectively. The presence of two unchanged
295 T_g values in the PM prepared from C971 and both POZ samples (50 and 500 kDa) is indicating
296 a phase separation of the polymers, i.e., confirmed that they were not molecularly miscible
297 (Moustafine et al., 2011, 2013). The IPCs of these polymers present an intermediate glass
298 transition of 128.3-128.9 °C, similar to the changes observed in other IPCs and IPECs formed
299 via hydrogen and ionic bonding, respectively (Khutoryanskiy et al, 2004b; Khutoryanskiy et
300 al, 2004c; Ruiz-Rubio et al., 2018; Mustafin, 2011; Mustafin et al., 2011, 2015; Moustafine et
301 al., 2011, 2013).

302 **(Figure 6 is here).**

303 5. Swelling properties

304 Swelling of the matrices in the media mimicking the gastrointestinal tract indicate that the
305 compacts based on POZ 50 kDa and POZ 500 kDa completely dissolved at the end of the first
306 hour (**Figure 7**). Matrices from C971 showed the highest values in swelling estimated by both
307 methods (**Figure 8a, b**). During swelling, the matrices separated into two clearly visible layers,
308 transparent external gel and non-hydrated white core. We believe that the external layer is
309 formed due to the hydration of macromolecules with ionized carboxyl groups, while the core
310 is still containing the chains with protonated COOH groups. Physical mixtures with POZ 50
311 kDa (PM-1) and POZ 500 kDa (denoted as PM-2) show the values of matrix size similar to
312 C971, but characterized by gradual release of POZ, localized in the external layer of the
313 matrices in buffer medium. On the contrary, the swelling profiles of PM-1 and PM-2 are similar
314 to each other only in acidic medium and have different character in the buffer at pH 6.8. The
315 PM matrices based on POZ 50 kDa have two times lower swelling index in the buffer medium,
316 compared to the swelling profile of PM with POZ 500 kDa. Moreover, in the case of two PM
317 samples containing POZ with different molecular weight a stable swelling profile was observed
318 only in the case of PM-1, relatively independent of the medium. PM-2 had a swelling profile
319 similar to the matrices composed of pure C971, but with three times lower swelling degree as
320 compared to the pure Carbopol[®]. These observations are believed to be resulting from
321 hydrogen bonding effect between these polymers, which was probably happened within PM
322 matrices under acidic conditions.

323 **(Figure 7 is here)**

324 Upon swelling, the polycomplex matrices showed the smaller dimensions, which means
325 lower swelling ability. Additionally, the swelling profiles of IPC matrices showed similar
326 character, but different swelling ability: in case of IPC formed with POZ 500 kDa the maximal
327 swelling was approximately two times greater compared to the IPC with POZ 50 kDa. So, only
328 PMs and IPCs with POZ 50 kDa show the most stable profiles with the lowest swelling degree,
329 but in case of PM it has three times lower degree of swelling. The formulations consisting of
330 proton-accepting non-ionic polymers (PVP, PEO, HPMC, HPC, MC, etc.) and proton-donating
331 polycarboxylic acids – (polyacrylic / polymethacrylic acids, Carbopol[®] grades) could form
332 IPCs under acidic pH and their swelling and drug release properties are controlled by three-
333 dimensional network structure, which was formed as a result of complex formation between
334 the polymers following water penetration into the matrix (Takayama and Nagai, 1987; Satoh
335 et al., 1989; Ozeki et al., 1998a, 1998b, 1999, 2000, 2005; Tan et al., 2001).

336 **(Figure 8 is here)**

337 For further analysis the matrices with gel layers and non-hydrated cores were taken out from
338 the dissolution baskets in GIT- mimicking media at different time intervals (0, 2 and 6 h); their
339 gel layers and non-hydrated cores were physically separated and freeze-dried. The algorithm
340 of their physicochemical analysis is schematically illustrated in **Figure 9**.

341 **(Figure 9 is here)**

342 ATR-FTIR spectra (**Figure 10**) were recorded to gain a deeper insight into the spatial
343 distribution of the macromolecules and their interactions in the matrix tablets containing PM
344 based on POZ and C971 following their hydration. In the intact interpolymer complex, a shift
345 of the C=O bands is observed to 1720 cm⁻¹, while the amide I band shifts to 1600 cm⁻¹. These
346 bands are related to hydrogen bonding between carboxyl groups of C971 and amide groups of
347 POZ.

348 **(Figure 10 is here)**

349 During the first 2 h in pH 1.2, the monolith polycomplex matrix has the composition
350 similar to IPC without any differences in FTIR spectra and *T_g* values; however, there is a slight
351 change in the composition of IPC from C971/POZ 1.4:1 into 1.5:1. During the swelling for 4
352 h in the buffer solution (pH 6.8), the gel layer is formed that is composed of mainly C971 in its
353 ionized hydrated form (appearance of a new band at 1557 cm⁻¹). In contrast, the amount of

354 POZ (according to the elemental analysis results, presented in **Table 1**) in the gel layer within
355 4 h (pH 6.8) is decreased and reached 2.7:1 C971/POZ molar ratio. This is also evidenced by
356 the presence of amide I stretching at 1633 cm^{-1} and the individual T_g value assigned to the pure
357 POZ at $45.1\pm 0.8\text{ }^\circ\text{C}$. Moreover, an increase in the T_g values from 125.2 ± 0.3 to $127.9\pm 0.7\text{ }^\circ\text{C}$
358 and observed shifts of the characteristic bands at 1600 to 1606 cm^{-1} are related to the presence
359 of hydrogen bonds between amide groups of POZ and carboxyl groups of C971; however, some
360 segments of the IPC contain partly ionized COO^- groups leading to dissociation of some
361 interpolymer bonds. On the contrary, the non-hydrated core of IPC matrices still consists of the
362 polycomplex structure, whose composition is close to the original IPC and IPC monolith matrix
363 taken after its exposure to the acidic medium (pH 1.2). This result agrees with our studies using
364 TEM technique.

365 **(Table 1 is here).**

366 The swelling behavior of PMs was found to be completely different from the tablets
367 based on IPCs. Clearly, POZ and C971 dispersed uniformly in the intact tablet prior to
368 hydration, as reflected by the presence of their characteristic peaks with high intensities in the
369 spectrum of PM, such as the peak of the carboxyl stretching band of C971 (1704 cm^{-1}) and a
370 “shoulder” of amide I of POZ (1633 cm^{-1}). According to above discussed mechanism of IPCs
371 formation and also the literature data (Takayama and Nagai, 1987; Satoh et al., 1989; Ozeki et
372 al., 1998a, 1998b; Tan et al., 2001; Zhang et al., 2016a, 2016b; Yusif et al., 2016; Szakonyi
373 and Zelko, 2016, Nguyen et al., 2016), the passage of the tablets through pH 1.2 media
374 facilitates strong interaction between the polymers. However, the spectral and thermal analysis
375 results did not provide any evidence for the complexation under these conditions: the band
376 corresponding to the self-associated carboxylic groups (COOH) located at 1704 cm^{-1} showed a
377 very minor shift to 1707 cm^{-1} and the presence of amide I stretching was observed at 1622 cm^{-1} ;
378 T_g values at $51.7\pm 0.9\text{ }^\circ\text{C}$ and $131.9\pm 0.8\text{ }^\circ\text{C}$ observed are assigned to the pure POZ 50 kDa
379 and C971, respectively. Moreover, some amount of pure POZ 50 kDa is leaching from the
380 matrices, so the composition of mixture is changed from C971/POZ 1.4:1 to 2.2:1.

381 During 4 h swelling of PM-1 in pH 6.8, the matrix composition becomes different to
382 the composition of IPC. As it is seen from the data presented in **Fig. 10** and **Table 1**, PM-1
383 with POZ 50 kDa tablets completely transformed to the transparent gel with maximal gel-
384 forming capacity, which is clearly visible compared to pure C971 matrix. Additionally, in the
385 ATR-FTIR spectrum of the freeze-dried gel layer (formed during 4 h swelling) the peak at

386 1704 cm^{-1} , corresponding to the carboxylic groups of C971, disappeared and was replaced by
387 a new band at 1556 cm^{-1} assigned to the carboxylate ion (COO^-). These findings indicated that
388 the carboxylic groups in C971 were ionized when it came to contact with pH 6.8 buffer. This
389 is also confirmed by higher T_g value (145.7 ± 0.7 °C) assigned to the ionized C971 that is in
390 good agreement with literature (Gomez-Carracedo et al., 2004). POZ was also present in the
391 gel layer: the peak at 1630 cm^{-1} corresponding to the amide I stretching and somehow higher
392 T_g value (59.4 ± 0.9 °C) were assigned to POZ. At 4 h in pH 6.8 (with a total swelling time of
393 6 h), the gel layer lost substantial amount of POZ, as confirmed by remarkable change in
394 C971/POZ composition from 1.4:1 to 5.8:1. So, the leaching of pure POZ from the gel layer is
395 evident. The diffusion of POZ from the gel layer led to increase in the diffusional path length
396 of the matrix, by which the drug release rate could be sustained (Ruiz-Rubio et al., 2018).

397 POZ was predominantly present in the non-hydrated core at 4 h of swelling, evidenced
398 by a strong band at 1627 cm^{-1} . In particular, the peak at 1704 cm^{-1} assigned to the self-
399 associated carboxylic groups of C971 exhibited a gradual increase in the intensity with time
400 and shifted to 1715 cm^{-1} corresponding to the carbonyl C=O stretching vibrations bands
401 (Takayama and Nagai, 1987; Satoh et al., 1989; Ozeki et al., 1998a, 1998b, 1999, 2000, 2005).
402 At 6 h of swelling, the non-hydrated core was completely transformed into hydrated form: T_g
403 value assigned to POZ at 45.2 ± 0.7 °C and slightly ionized C971 at 140.4 ± 0.9 °C. Composition
404 of the material after complete hydration also changed from C971/POZ 1.4:1 to 2.4:1.

405 In addition, a frequency shift in the peak assigned to the amide I stretching group of
406 POZ in the gel layer and non-hydrated core at 6 h of swelling changed from 1633 cm^{-1} to 1600
407 cm^{-1} and appearance of characteristic T_g value at 125.2 ± 0.3 °C, typical for strong hydrogen
408 bonding between POZ and C971 were not observed.

409 6. Drug release studies

410 Mesalazine (5-ASA) is an anti-inflammatory drug that is used to treat some conditions of
411 gastrointestinal tract, for example, inflammatory bowel disease (Quinteros et al, 2010). 5-ASA
412 was used in this work as a model drug. The release of 5-ASA from the matrices was evaluated
413 under GIT mimicking conditions. **Figure 11** shows the dissolution profiles from the matrices
414 based on C971 as well as their IPCs and PMs with POZ. Drug released faster from the matrices
415 composed of pure POZ (RR=0.8513 %/min and 0.6665 %/min for 50 and 500 kDa POZ,
416 respectively) and IPCs (RR=0.3676 %/min and 0.9016 %/min for 50 and 500 kDa POZ,
417 respectively) compared to pure C971 (RR=0.1644 %/min) and PMs (0.1017 %/min and 0.1610

418 %/min for 50 and 500 kDa POZ, respectively). Moreover, IPCs with POZ 500 kDa show faster
419 release in acidic medium compared to all other samples. Additionally, the whole release
420 process for this IPC is finished during the first 2 h in acidic medium. Understanding of this
421 observation could come from our TEM results and evaluation of the swelling data. According
422 to TEM data, under strongly acidic conditions the dense IPC particles with POZ 500 kDa are
423 formed and their size reaches 649 ± 185 nm (pH 2.14). Thus, in our release media (pH 1.2) the
424 IPC particles became bigger that leads to formation of greater pores in the system compared to
425 the IPC formed with POZ 50 kDa. Further evidence comes from the swelling properties of
426 polycomplex matrices. The swelling index, estimated by two methods shows that IPC with
427 POZ 500 kDa matrices exhibits greater swelling at pH 1.2 compared to IPC with POZ 50 kDa
428 due to the formation of compact monolith structure with much lower porosity. Moreover, the
429 observed phenomena also indicate that POZ is predominantly present on the surface of
430 microgels formed from weakly cross-linked C971.

431 Despite that diffusion of POZ 500 kDa from non-hydrated core to the gel layer may be slower
432 due to its high molecular weight, compared to PM made from POZ 50 kDa, drug release process
433 may proceed differently. It is known that hydrogen bonds in IPC matrices help increasing the
434 gel strength to improve the release-retarding capacity of polymer matrix (Tan et al., 2001;
435 Zhang et al., 2015, 2016; Yusif et al., 2016; Szakonyi and Zelko, 2016, Nguyen et al., 2016).
436 Thus, in case of some proton-accepting non-ionic polymers (e.g. hydroxypropyl cellulose,
437 HPC) and polycarboxylic acids (PAA or Carbopols), which could form IPC in acidic pH region
438 and of course, in typical dissolution media, the release of drugs is controlled by the three-
439 dimensional network structure, which is affected by complex formation between these
440 polymers following water penetration into the matrix (Satoh et al, 1989). If it can happen we
441 will see a significant retardation of drug release, but mostly in the case of PM matrices and not
442 for IPCs.

443 The release rate of 5-ASA greatly decreases when the matrix was composed of PM. According
444 to the abovementioned explanation of the swelling results, the decrease in the release rate in
445 this case could be due to the complexation between the polymers, which has happened inside
446 the matrix during penetration of dissolution media, resulting in the formation of three-
447 dimensional network. This leads to the formation of insoluble fibers in the matrix structure,
448 which significantly retard the drug release process.

449 **(Figure 11 is here)**

450 Based on these results, the following explanation of drug release from IPC system could be
451 proposed: in acidic medium, macromolecules of IPC swell significantly and 5-ASA partially
452 dissolves from the surface of the matrix. The remaining amount of the undissolved drug after
453 its transfer to another medium could continuously dissolve and diffuse from the swollen gel
454 layer, that acts as a driving force for 5-ASA molecules. On the contrary, at pH 6.8, hydrogen
455 bonds between POZ and C971 are dissociated due to gradual ionization of COOH groups of
456 C971 and 5-ASA, leading to destruction of interpolymer contacts (according to FTIR and
457 mDSC data). Together with release of free POZ macromolecules (according to elemental
458 analysis data) this facilitates dissolution of 5-ASA. Hence, C971 was responsible for sustaining
459 drug release during the first 2 h to prevent the initial burst release. POZ then diffused gradually
460 from the non-hydrated core to the gel layer, decreasing the gel strength and resulting in the
461 gradual destruction of hydrogen bonding interaction between POZ and C971. For this reason,
462 the rate of 5-ASA release in this polymer system (mixture-loaded matrix) progressively
463 increased at latter stages.

464 Additionally, drug release from different matrices could also be affected by specific
465 interactions of mesalazine with C971 and POZ. As 5-ASA contains both proton-donating and
466 proton-accepting groups in its structure, its interaction with Carbopols via ionic contacts
467 (Quinteros et al, 2011) and with POZ via hydrogen bonding could not be ruled out completely.
468 pH of dissolution medium is also expected to have effect on these interactions.

469

470 **Conclusions**

471 Formation of interpolymer complexes between Carbopol[®] 971 and poly(2-ethyl-2-oxazoline)
472 of different molecular weights has been studied in aqueous solutions at different pHs. It was
473 established that interpolymer hydrogen bonding is responsible for this complex formation;
474 these interactions are possible only under acidic conditions. The evolution in the structure of
475 the products of interpolymer interaction was studied in solutions with different pH. Upon a
476 gradual decrease in solution pH the polymer mixtures evolved from completely non-interacting
477 macromolecules to initial interpolymer associates, which then converted into primary compact
478 IPC particles that were eventually transformed into spherical aggregates. Tablets were then
479 prepared from interpolymer complexes and physical mixtures of Carbopol[®] 971 and poly(2-
480 ethyl-2-oxazoline) with and without a model drug (mesalazine). The structure of these
481 materials was evaluated using FTIR and differential scanning calorimetry methods as well as
482 swelling studies in the media mimicking conditions of gastrointestinal tract. It was established

483 that the state of the polymers in the mixture and their swelling behavior is affected by the
484 possibility of the complexation between them. The release of mesalazine from these tablets is
485 also strongly influenced by the presence of interpolymer complexation. To the best of our
486 knowledge, this is the first time when interpolymer complexes between Carbopol® 971 and
487 poly(2-ethyl-2-oxazoline) were used to prepare solid dosage forms for gastrointestinal drug
488 delivery. Potentially future research could compare poly(2-ethyl-2-oxazoline) with other non-
489 ionic polymers capable of forming interpolymer complexes with Carbopol® 971 (e.g.
490 polyvinylpyrrolidone and polyethylene oxide) to establish if it could offer any advantages as a
491 novel pharmaceutical excipient.

492

493 **Acknowledgments**

494 This work was, in part, financially supported by the Russian Foundation for Basic Research
495 (RFBR) and the Russian Science Foundation (RSF) in the framework of projects 16-04-01692
496 (to R.I.M.) and 14-15-01059 (to R.I.M., A.S.V.), respectively. The authors acknowledge the
497 Ministry of Education and Science of the Republic of Tatarstan (Russia) for “Algarysh” grant
498 supporting V.V.K. visits to Kazan State Medical University. Chemical Analysis Facility
499 (University of Reading) and Dr Peter Harris are gratefully acknowledged for access to
500 transmission electron microscopy and for provision of technical help. The authors are also
501 grateful to Mr Shamil Nasibullin for his technical help with thermal analysis.

502

503 **References**

504 Ambreen J., Siddiq M. (2014). Effect of arm number of poly(acrylic acid) on cloud point
505 temperature of poly(2-ethyl-2-oxazoline). *J. Polym. Res.* 21, 608.

506 Bekturov E.A., Bimendina L.A. (1981). Interpolymer complexes. *Adv. Polym. Sci.* 41, 99-147.

507 Bludau H., Czapar A.E., Pitek A.S., Shukla S., Jordan R., Steinmetz N.F. (2017). POxylation
508 as an alternative stealth coating for biomedical applications. *Eur. Polym. J.*, 88, 679-688.

509 Christova D., Velichkova R., Loos W., Goethals E.J., Du Prez F. (2003). New thermo-
510 responsive polymer materials based on poly(2-ethyl-2-oxazoline) segments. *Polymer*, 44,
511 2255–2261.

512 Claeys B., Vervaeck A., Vervaeet C., Remon J.P., Hoogenboom R., De Geest B.G. (2012).
513 Poly(2-ethyl-2-oxazoline) as matrix excipient for drug formulation by hot melt extrusion and
514 injection molding. *Macromol. Rapid Commun.*, 33, 1701-1707.

515 Dai J., Goh S.H., Lee S.Y., Siow K.S. (1994). Complexation between poly(2-
516 hydroxypropylmethacrylate) and three tertiary amide polymers. *J. Appl. Polym. Sci.* 53, 837-
517 845.

518 de la Rosa V.R. (2014). Poly(2-oxazoline)s as materials for biomedical applications. *J. Mater.*
519 *Sci.: Materials in Medicine*, 25, 1211–1225.

520 Diehl C., Schlaad H. (2009). Thermo-responsive polyoxazolines with widely tuneable LCST.
521 *Macromol Biosci.* 9, 157-161.

522 Fael H., Rafols C., Demirel A.L. (2018). Poly(2-ethyl-2-oxazoline) as an alternative to
523 poly(vinylpyrrolidone) in solid dispersions for solubility and dissolution rate enhancement of
524 drugs. *J. Pharm. Sci.* 107, 2428-2438.

525 Farrugia B.L, Kempe K., Schubert U.S., Hoogenboom R., Dargaville T.R. (2013). Poly(2-
526 oxazoline) Hydrogels for Controlled Fibroblast Attachment. *Biomacromolecules*, 14, 2724-
527 2732.

528 Filippov S.K., Verbraeken B., Konarev P.V., Svergun D.I, Angelov B., Vishnevetskaya N.S.,
529 Papadakis C.M., Rogers S., Radulescu A., Courtin T., Martins J.C., Starovoytova L., Hruba
530 M., Stepanek P., Kravchenko V.S., Potemkin I.I., Hoogenboom R. (2017). Block and Gradient
531 Copoly(2-oxazoline) Micelles: Strikingly Different on the Inside. *J. Phys. Chem. Lett.*, 8,
532 3800–3804.

533 Garipova V.R., Gennari C.G.M., Selmin F., Cilurzo F., Moustafine R.I. (2018). Mucoadhesive
534 interpolyelectrolyte complexes for the buccal delivery of Clobetasol, *Polymers*, 10(1), 85.

535 Gomez-Carracedo A., Alvarez-Lorenzo C., Gomez-Amoza J.L., Concheiro A. (2004). Glass
536 transitions and viscoelastic properties of Carbopol[®] and Noveon[®] compacts, *Int. J. Pharm.* 274,
537 233-243.

538 Hoogenboom R. (2009). Poly(2-oxazoline)s: A Polymer Class with Numerous Potential
539 Applications. *Angew. Chem. Int. Ed.*, 48, 7978 – 7994

540 Hoogenboom R., Schlaad H. (2017). Thermoresponsive poly(2-oxazoline)s, polypeptoids, and
541 polypeptides. *Polym. Chem.*, 8, 24–40.

542 Hruby M., Filippov S.K., Panek J., Novakova M., Mackova H., Kucka J., Vetvicka D., Ulbrich
543 K. (2010). Polyoxazoline thermoresponsive micelles as radionuclide delivery systems.
544 *Macromol Biosci.* 10, 916-924.

545 Isasi J.R., Meaurio E., Cesteros C., Katime I. (1996). Miscibility and specific interactions in
546 blends of poly(2-ethyl-2-oxazoline) with hydroxylated polymethacrylates. *Macromol. Chem.*
547 *Phys.* 197, 641-649.

548 Kemenova V.A., Mustafin (Moustafine) R.I., Alekseyev K.V., Scorodinskaya A.M., Zezin
549 A.B., Tencova A.I., Kabanov V.A. (1991). Applying interpolymer complexes in pharmacy.
550 *Farmatsiya* 60(1), 67–72.

551 Kharlampieva E., Kozlovkaya V., Sukhishvili S.A. (2009). Layer-by-Layer Hydrogen-Bonded
552 Polymer Films: From Fundamentals to Applications. *Adv. Mater.*, 21, 3053–3065

553 Khutoryanskaya O.V., Williams A.C., Khutoryanskiy V.V. (2007). pH-mediated interactions
554 between poly(acrylic acid) and methylcellulose in the formation of ultrathin multilayered
555 hydrogels and spherical nanoparticles, *Macromolecules*, 40, 7707-7713.

556 Khutoryanskiy V.V., Mun G.A., Nurkeeva Z.S., Dubolazov A.V. (2004a). pH- and salts-
557 effects on interpolymer complexation via hydrogen bonding in aqueous solutions, *Polym. Int.*,
558 53, 1946-1950.

559 Khutoryanskiy V.V., Dubolazov A.V., Nurkeeva Z.S., Mun G.A. (2004b). pH-effects in the
560 complex formation and blending of poly(acrylic acid) with poly(ethylene oxide), *Langmuir* 20,
561 9, 3785-3790.

562 Khutoryanskiy V.V., Cascone M.G., Lazzeri L., Barbani N., Nurkeeva Z.S., Mun G.A.,
563 Dubolazov A.V. (2004c). Morphological and thermal characterization of interpolymer
564 complexes and blends based on poly(acrylic acid) and hydroxypropylcellulose, *Polym. Int.* 53,
565 307–311.

566 Khutoryanskiy V.V. (2007). Hydrogen-bonded interpolymer complexes as materials for
567 pharmaceutical applications. *Int. J. Pharm.* 334, 15-26.

568 Khutoryanskiy V.V. (2018). Beyond PEGylation: alternative surface-modification of
569 nanoparticles with mucus-inert biomaterials, *Advanced Drug Delivery Reviews*, 124, 140-149.

570 Kim C., Lee S.C., Kwon I.C., Chung H., Jeong S.Y. (2002). Complexation of poly(2-ethyl-2-
571 oxazoline)-block-poly(ϵ -caprolactone) micelles with multifunctional carboxylic acids.
572 *Macromolecules*, 35, 193-200.

573 Lehner R., Liu K., Wang X., Wolf M., Hunziker P. (2017). A comparison of plasmid DNA
574 delivery efficiency and cytotoxicity of two cationic diblock polyoxazoline copolymers.
575 *Nanotechnology* 28, 175602, 1-11.

576 Lorson T., Lübtow M.M., Wegener E., Haider M.S., Borova S., Nahm D., Jordan R., Sokolski-
577 Papkov M., Kabanov A.V., Luxenhofer R. (2018). Poly(2-oxazoline)s based biomaterials: A
578 comprehensive and critical update. *Biomaterials*. 178, 204-280.

579 Luxenhofer R., Han Y., Schulz A., Tong J., He Z., Kabanov A.V., Jordan R. (2012). Poly(2-
580 oxazoline)s as polymer therapeutics. *Macromol Rapid Commun.* 33, 1613-1631.

581 Mansfield E.D.H., de la Rosa V.R., Kowalczyk R.M., Grillo I., Hoogenboom R., Sillence K.,
582 Hole P., Williams A.C., Khutoryanskiy V.V. (2016). Side chain variations radically alter the
583 diffusion of poly(2-alkyl-2-oxazoline)s functionalised nanoparticles through a mucosal barrier,
584 *Biomat. Sci.*, 4, 1318-1327.

585 Mansfield E.D.H., Sillence K., Hole P., Williams A.C., Khutoryanskiy V.V. (2015).
586 POZylation; a new approach to enhance nanoparticle diffusion through mucosal barriers,
587 *Nanoscale*, 7, 13671-13679.

588 Mero A., Pasut G., Via L.D., Fijten M.W.M., Schubert U.S., Hoogenboom R., Veronese F.M.
589 (2008). Synthesis and characterization of poly(2-ethyl 2-oxazoline)-conjugates with proteins
590 and drugs: Suitable alternatives to PEG-conjugates? *J. Control. Release*, 125, 87–95.

591 Moustafine R.I., Bobyleva V.L., Bukhovets A.V., Garipova V.R., Kabanova T.V., Kemenova
592 V.A., Van den Mooter G., (2011). Structural transformations during swelling of polycomplex
593 matrices based on countercharged (meth)acrylate copolymers (Eudragit[®] E PO/Eudragit[®] L
594 100-55). *J. Pharm. Sci.*, 100(3), 874-885.

595 Moustafine R.I., Bukhovets A.V., Sitenkov A.Y., Kemenova V.A., Rombaut P., Van den
596 Mooter G. (2013). Eudragit[®] E PO as a complementary material for designing oral drug
597 delivery systems with controlled release properties: comparative evaluation of new
598 interpolyelectrolyte complexes with countercharged Eudragit[®] L100 copolymers. *Mol. Pharm.*,
599 10(7), 2630–2641.

600 Moustafine R.I., Zaharov I.M., Kemenova V.A. (2006). Physicochemical characterization and
601 drug release properties of Eudragit[®] EPO/Eudragit[®] L 100-55 interpolyelectrolyte complexes.
602 Eur. J. Pharm. Biopharm. 63, 26–36.

603 Mun G.A., Nurkeeva Z.S., Khutoryanskiy V.V., Bitekenova A.B. (2000). Effect of copolymer
604 composition on interpolymer complex formation of (co)polyvinyl ethers with polyacrylic acid
605 in aqueous and organic solutions, Macromol. Rapid Commun., 21, 381-384.

606 Mustafin R.I. (Moustafine R.I.), (2011). Interpolymer combinations of chemically
607 complementary grades of Eudragit copolymers: A new direction in the design of peroral solid
608 dosage forms of drug delivery systems with controlled release (review). Pharm. Chem. J. 45,
609 285-295.

610 Mustafin R.I. (Moustafine R.I.), Bukhovets A.V., Sitenkov A.Yu., Garipova V.R., Kemenova
611 V.A., Rombaut P., Van den Mooter G. (2011). Synthesis and characterization of a new carrier
612 based on Eudragit[®] EPO/S100 interpolyelectrolyte complex for controlled colon-specific drug
613 delivery. Pharm. Chem. J. 45, 568-574.

614 Mustafin R.I. (Moustafine R.I.), Semina I. I., Garipova V.R., Bukhovets A.V., Sitenkov
615 A.Yu., Salakhova A.R., Gennari C.G.M., Cilurzo F. (2015). Comparative study of
616 polycomplexes based on Carbopol[®] and oppositely charged polyelectrolytes as a new oral drug
617 delivery system. Pharm. Chem. J. 49(1), 1-6.

618 Nguyen H.V., Nguyen V.H., Lee B.-J. (2016). Dual release and molecular mechanism of
619 bilayered aceclofenac tablet using polymer mixture. Int. J. Pharm., 515, 233-244.

620 Nurkeeva Z.S., Mun G.A., Dubolazov A.V., Khutoryanskiy V.V. (2005). pH-effects on the
621 complexation, miscibility and radiation-induced cross-linking in poly(acrylic acid)-poly(vinyl
622 alcohol) blends, Macromol. Biosci., 5, 424-432.

623 Nurkeeva Z.S., Mun G.A., Khutoryanskiy V.V., Bitekenova A.B., Dubolazov A.V.,
624 Esirkegenova S.Zh. (2003). pH effects in the formation of interpolymer complexes between
625 poly(N-vinylpyrrolidone) and poly(acrylic acid) in aqueous solutions, Eur. Phys. J. E, 10, 65-
626 68.

627 Ozeki T., Yuasa H., Kanaya Y. (1998a). Control of medicine release from solid dispersion
628 through poly(ethylene oxide)-carboxyvinyl polymer interaction. Int. J. Pharm., 165, 239-244.

629 Ozeki T., Yuasa H., Kanaya Y. (1998b). Mechanism of medicine release from solid dispersion
630 composed of poly(ethylene oxide)-carboxyvinylpolymer interpolymer complex and pH effect
631 on medicine release. *Int. J. Pharm.* 171, 123-132.

632 Ozeki T., Yuasa H., Kanaya Y. (1999). Controlled release from solid dispersion composed of
633 poly(ethylene oxide)-carboxyvinylpolymer interpolymer complex by varying molecular
634 weight of poly(ethylene oxide). *J. Control. Release* 58, 87-95.

635 Ozeki T., Yuasa H., Kanaya Y. (2000). Controlled release from solid dispersion composed of
636 poly(ethylene oxide)-carboxyvinylpolymer interpolymer complex with various cross-linking
637 degree of Carbopol®. *J. Control. Release* 63, 287-295.

638 Ozeki T., Yuasa H., Okada H. (2005). Controlled release of drug via methylcellulose-
639 carboxyvinylpolymer interpolymer complex solid dispersion. *AAPS PharmSciTech.* 6, e231-
640 e236.

641 Policianova O., Brus J., Hruby M., Urbanova m., Zhigunov A., Kredatusova J., Kobera L.
642 (2014). Structural diversity of solid dispersions of acetylsalicylic acid as seen by solid-state
643 NMR. *Mol. Pharm.*, 11, 516-530.

644 Quinteros D.A., Manzo R.H., Allemandi D.A. (2010). Design of a colonic delivery system
645 based on cationic polymethacrylate (Eudragit E100)-mesalamine complexes. *Drug Delivery*,
646 17(4): 208–213.

647 Quinteros D.A., Manzo R.H., Allemandi D.A. (2011). Interaction between Eudragit E100 and
648 anionic drugs: Addition of anionic polyelectrolytes and their influence on drug release
649 performance. *J. Pharm. Sci.*, 100(11): 4664-4673.

650 Ruiz-Rubio L., Alonso M.L., Pérez-Álvarez L., Alonso R.M., Vilas J.L., Khutoryanskiy V.V.
651 (2018). Formulation of Carbopol®/Poly(2-ethyl-2-oxazoline)s mucoadhesive tablets for buccal
652 delivery of hydrocortisone. *Polymers*, 10(2), 175.

653 Satoh K., Takayama K., Machida Y., Suzuki Y., Nakagaki M., Nagai T. (1989). Factors
654 affecting the bioadhesive properties property of tablets consisting of hydroxypropyl cellulose
655 and carboxyvinyl polymer. *Chem. Pharm. Bull.* 37, 1366-1368.

656 Su C., Ma S.-M., Liu G.-X., Yang S.-G. (2018). Dewetting behaviour of hydrogen bonded
657 polymer complex film under hydrothermal condition. *Chinese J. Polym. Sci.* 36, 1036-1042.

658 Su C., Sun J., Zhang X., Shen D., Yang S. (2017). Hydrogen-bonded polymer complex thin
659 film of poly(2-oxazoline) and poly(acrylic acid). *Polymers*, 9, 363.

660 Szakonyi G., Zelko R. (2016). Carbopol® - crospovidone interpolymer complex for pH-
661 dependent desloratadine release. *J. Pharm. Biomed. Anal.* 123, 141-146.

662 Takayama K., Nagai T. (1987). Application of interpolymer complexation of
663 polyvinylpyrrolidone/carboxyvinyl polymer to control of drug release *Chem. Pharm. Bull.*,
664 35(12), 4921-4927.

665 Takayama K., Hirata M., Machida Y., Masada T., Sannan T., Nagai T. (1990). Effect of
666 interpolymer complex formation on bioadhesive property and drug release phenomenon of
667 compressed tablet consisting of chitosan and sodium hyaluronate. *Chem. Pharm. Bull.* 38,
668 1993-1997.

669 Tan Y.T., Peh K.K., Al-Hanba O. (2001). Investigation of interpolymer complexation between
670 Carbopol and various grades of polyvinylpyrrolidone and effects on adhesion strength and
671 swelling properties. *J. Pharm. Pharm. Sci.* 4, 7-14.

672 Viegas T.X., Bentley M.D., Harris J.M., Fang Z., Yoon K., Dizman B., Weimer R., Mero A.,
673 Pasut G., Veronese F.M. (2011). Polyoxazoline: Chemistry, Properties, and Applications in
674 Drug Delivery. *Bioconj. Chem.*, 22, 976–986.

675 Yusif R.M., Abu Hashim I.I., Mohamed E.A., El Rakhawy M.M. (2016). Investigation and
676 evaluation of an in situ interpolymer complex of Carbopol with polyvinylpyrrolidone as a
677 matrix for gastroretentive tablets of ranitidine hydrochloride. *Chem. Pharm. Bull.* 64, 42-51.

678 Zhang F., Lubach J., Watson N.A. Momin S. (2016a). Interpolymer complexation between
679 Polyox and Carbopol on drug release from matrix tablets. *J. Pharm. Sci.* 105, 2386-2396.

680 Zhang F., Meng F., Lubach J., Koleng J., Watson N.A. (2016b). Properties and mechanisms of
681 drug release from matrix tablets containing poly(ethylene oxide) and poly(acrylic acid) as
682 release retardants. *Eur. J. Pharm. Biopharm.* 105, 97-105.

683 Zhunuspayev D.E., Mun G.A., Hole P., Khutoryanskiy V.V. (2008). Solvent effects on the
684 formation of nanoparticles and multi-layered coatings based on hydrogen-bonded interpolymer
685 complexes of poly(acrylic acid) with homo- and copolymers of N-vinyl pyrrolidone. *Langmuir*,
686 24, 13742-13747.

687

List of Tables and Figures

Table 1. Results of elemental, spectroscopic and thermal analysis of samples after swelling in the media mimicking gastro-intestinal tract conditions.

692

Figure 1. Turbidity of solution mixtures of Carbopol® 971 and POZ at different unit-molar ratios. Concentrations of Carbopol® 971 and POZ are 0.002 unit-mol/L.

Figure 2. Proposed scheme of complexation between Carbopol® 971 and POZ via hydrogen bonding.

Figure 3. Turbidity of 1:1 unit-mol solution mixtures of Carbopol® 971 and POZ as a function of pH. Concentrations of Carbopol® 971 and POZ are 0.01 unit-mol/L.

Figure 4. TEM images of IPCs prepared by mixing 0.01 unit-base mol/L solutions of Carbopol® 971 and POZ (500 kDa) in 1:1 unit-base molar ratio and adjusting pH by addition of HCl (a); Proposed mechanism of IPC formation at different pHs (b).

Figure 5. FTIR spectra of IPC (C971:POZ 50 kDa), physical mixture (C971:POZ 50 kDa), and individual C971 and POZ 50 kDa.

Figure 6. DSC thermograms of: (a) IPC (C971:POZ 50 kDa); physical mixture (C971:POZ 50 kDa); C971; POZ 50 kDa, (b) IPC (C971:POZ 500 kDa); physical mixture (C971:POZ 500 kDa); C971; and POZ 500 kDa.

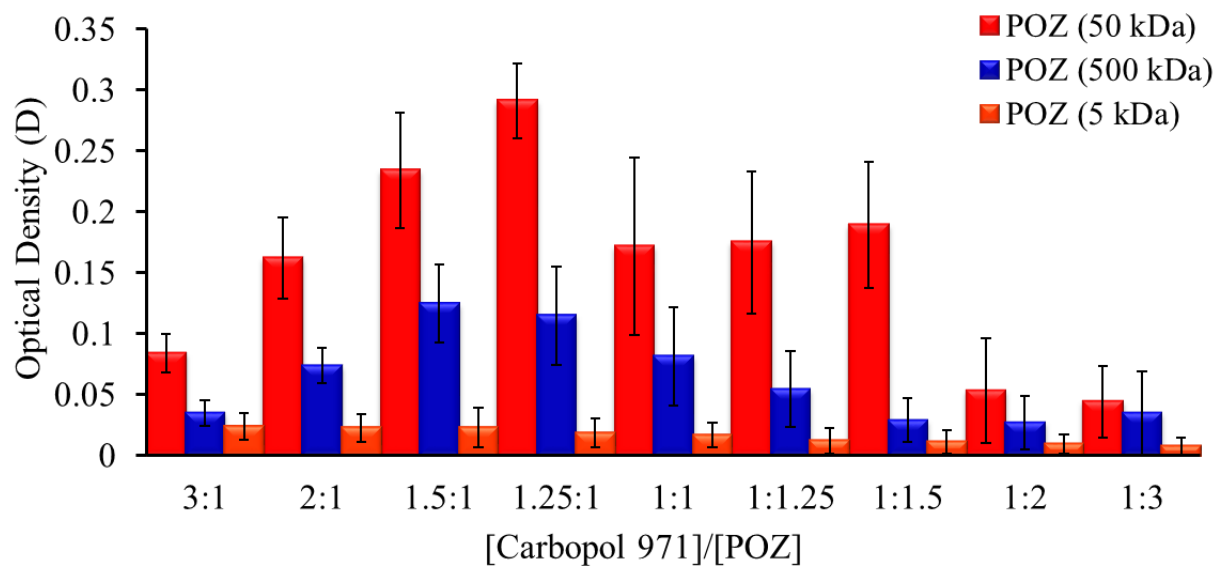
Figure 7. Comparison of swelling profiles of different matrices in the media mimicking gastro-intestinal tract conditions.

Figure 8. Changes in the external appearance of different matrices during swelling test (a): images and resulting matrix diameters generated through the image analysis (b).

Figure 9. Schematic representation of the physicochemical analysis of samples after swelling in the media mimicking gastro-intestinal tract conditions.

Figure 10. FTIR spectra of IPC based on POZ 50 kDa and C 971 after swelling in the media mimicking gastro-intestinal tract conditions.

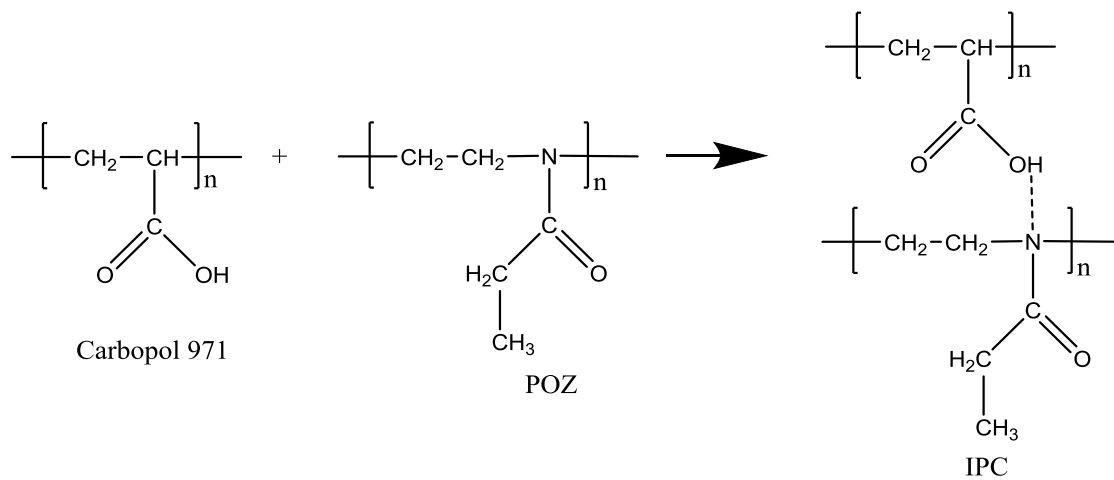
Figure 11. Release profiles of mesalazine from matrix systems under the conditions mimicking the gastro-intestinal tract.



719

720 **Figure 1.** Turbidity of solution mixtures of Carbopol® 971 and POZ at different unit-molar
 721 ratios. Concentrations of Carbopol® 971 and POZ are 0.002 unit-mol/L.

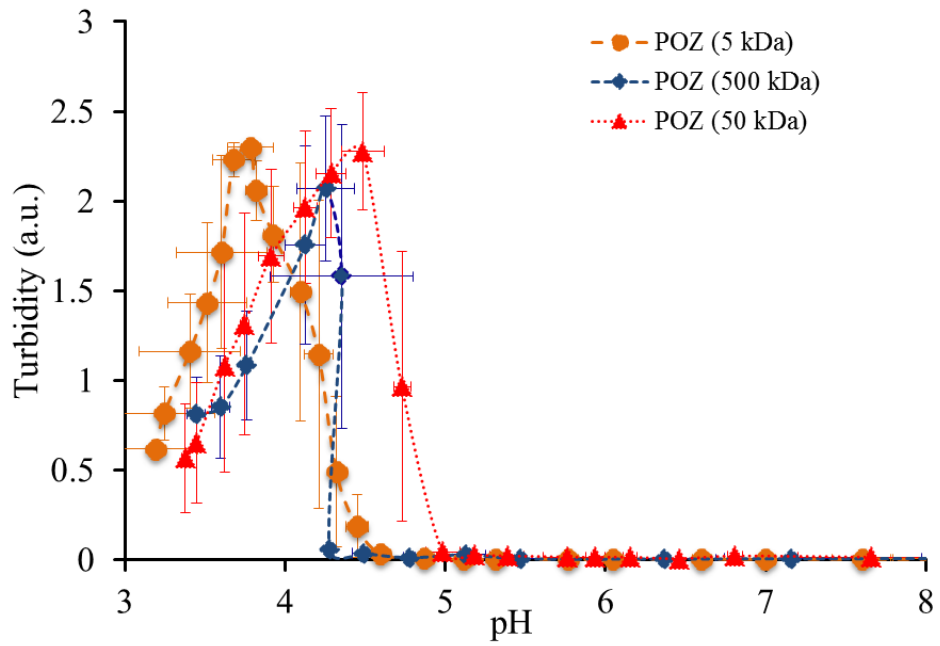
722



723

724 **Figure 2.** Proposed scheme of complexation between Carbopol® 971 and POZ via hydrogen
 725 bonding.

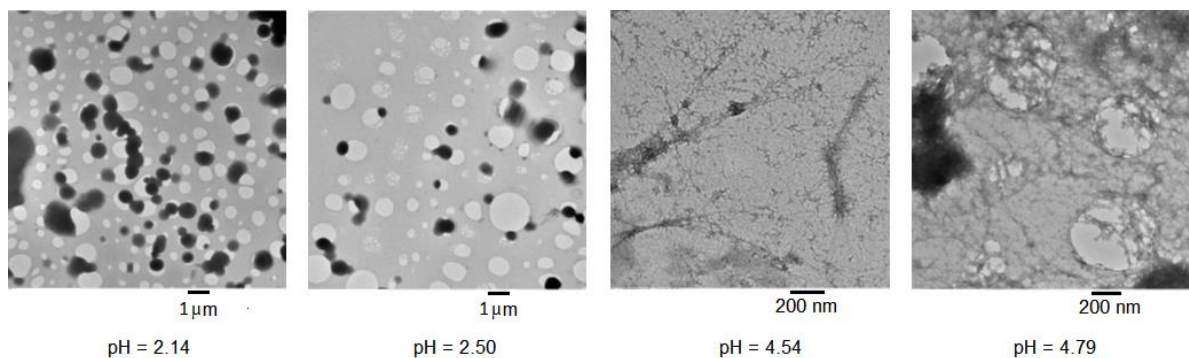
726



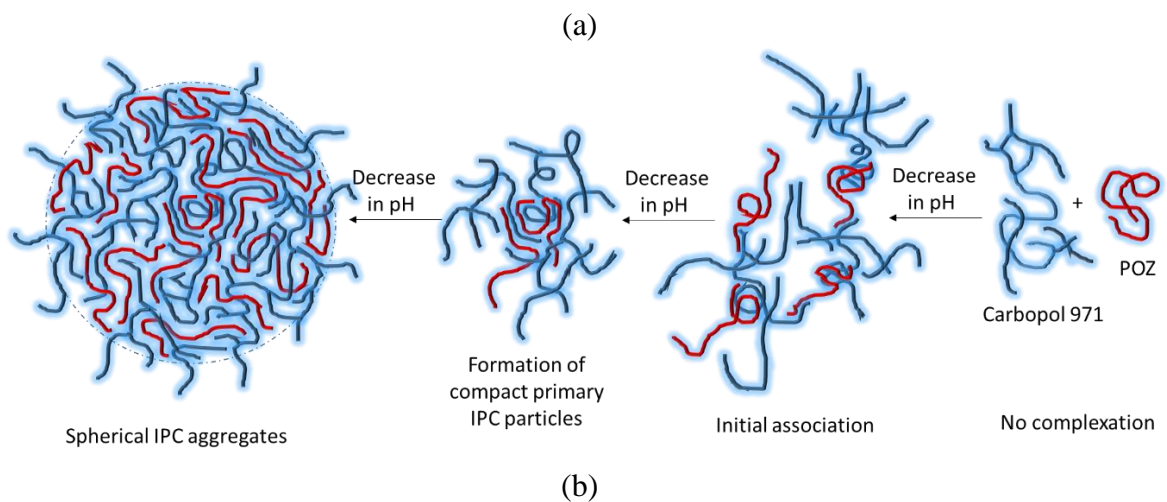
727

728 **Figure 3.** Turbidity of 1:1 unit-mol solution mixtures of Carbopol® 971 and POZ as a function
 729 of pH. Concentrations of Carbopol® 971 and POZ are 0.01 unit-mol/L.

730



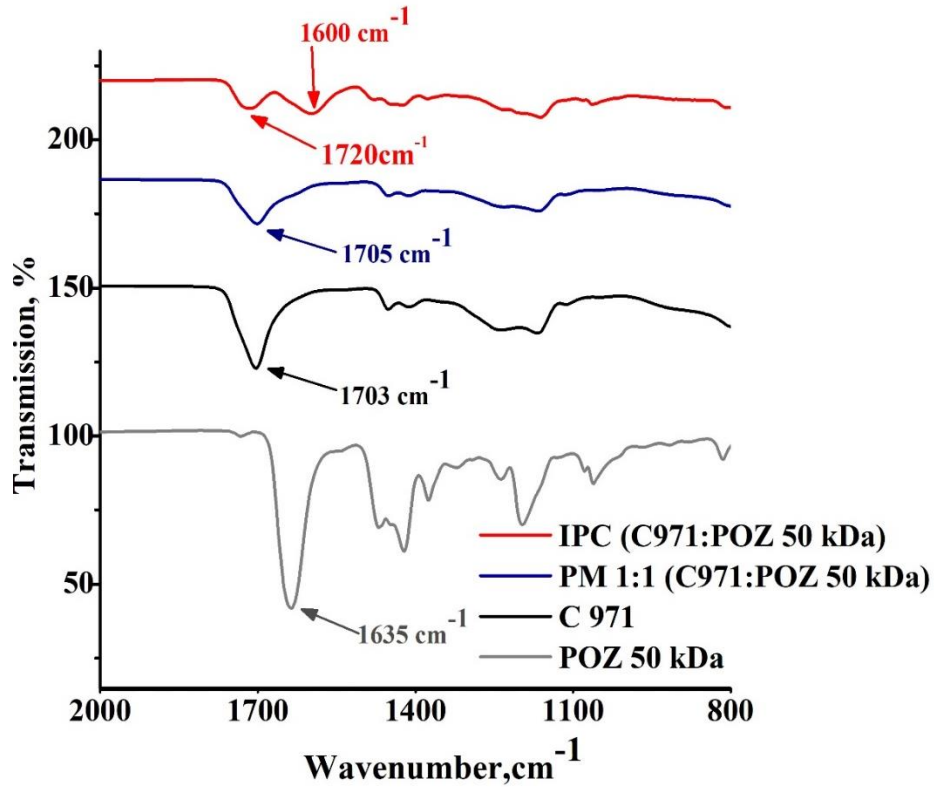
731
732



733
734

735 **Figure 4.** TEM images of IPCs prepared by mixing 0.01 unit-base mol/L solutions of
736 Carbopol® 971 and POZ (500 kDa) in 1:1 unit-base molar ratio and adjusting pH by addition
737 of HCl (a); Proposed mechanism of IPC formation at different pHs (b).

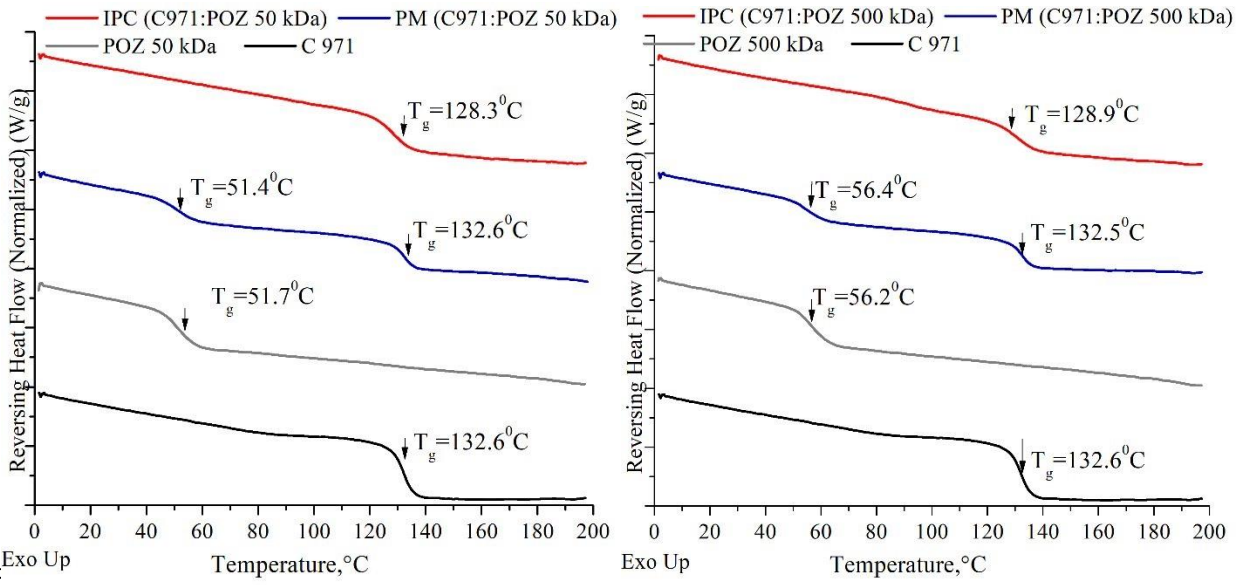
738



739

740 **Figure 5.** FTIR spectra of IPC (C971:POZ 50 kDa), physical mixture (C971:POZ 50 kDa),
741 and individual C971 and POZ 50 kDa.

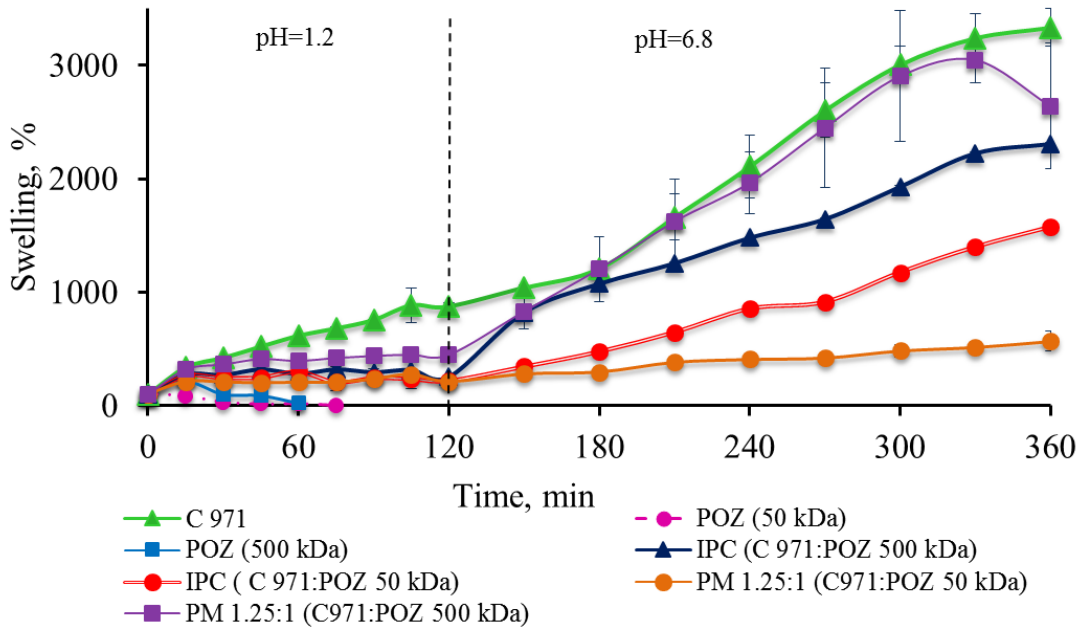
742



(a)

(b)

Figure 6. DSC thermograms of: (a) IPC (C971:POZ 50 kDa); physical mixture (C971:POZ 50 kDa); C971; POZ 50 kDa, (b) IPC (C971:POZ 500 kDa); physical mixture (C971:POZ 500 kDa); C971; POZ 500 kDa.

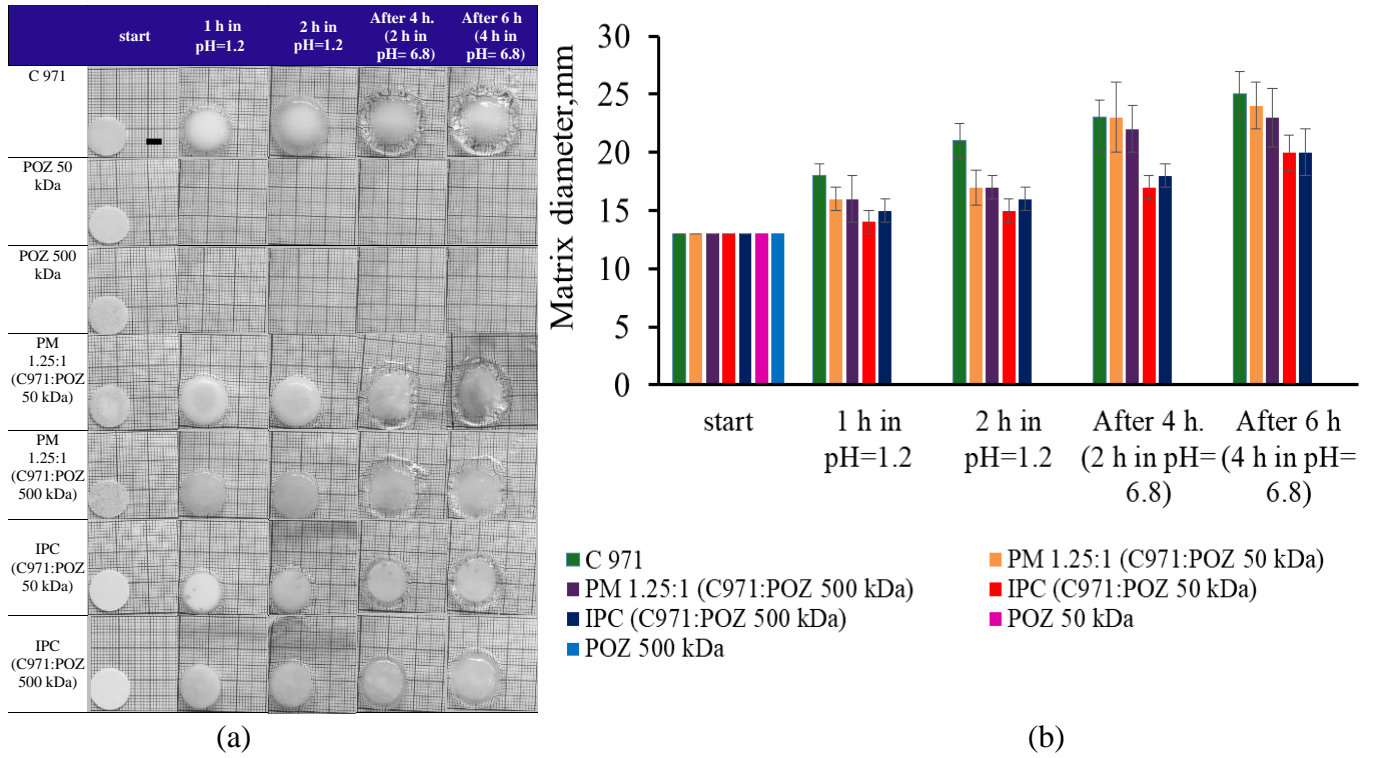


752

753

754 **Figure 7.** Comparison of swelling profiles of different matrices in the media mimicking gastro-
 755 intestinal tract conditions.

756



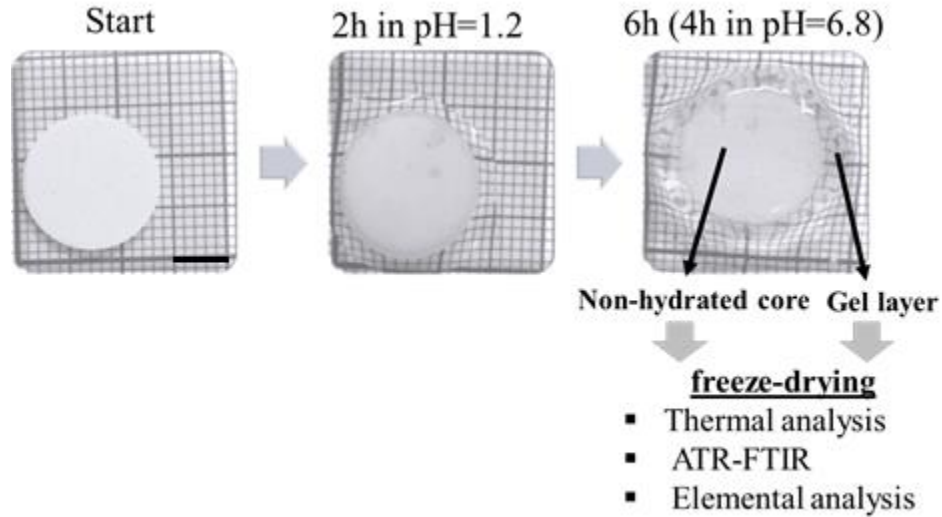
757

758

759 **Figure 8.** Changes in the external appearance of different matrices during swelling test (a):
 760 images and resulting matrix diameters generated through the image analysis (b). Scale bar is 5
 761 mm

762

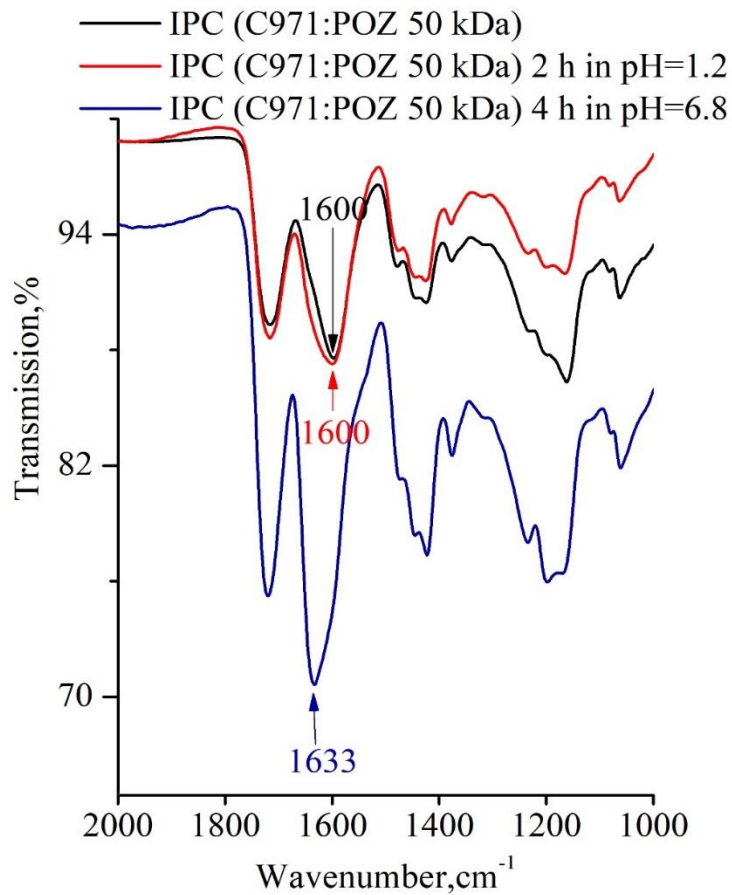
763



764

765 **Figure 9.** Schematic representation of the physicochemical analysis of samples after swelling
 766 in the media mimicking gastro-intestinal tract conditions. Scale bar is 5 mm

767

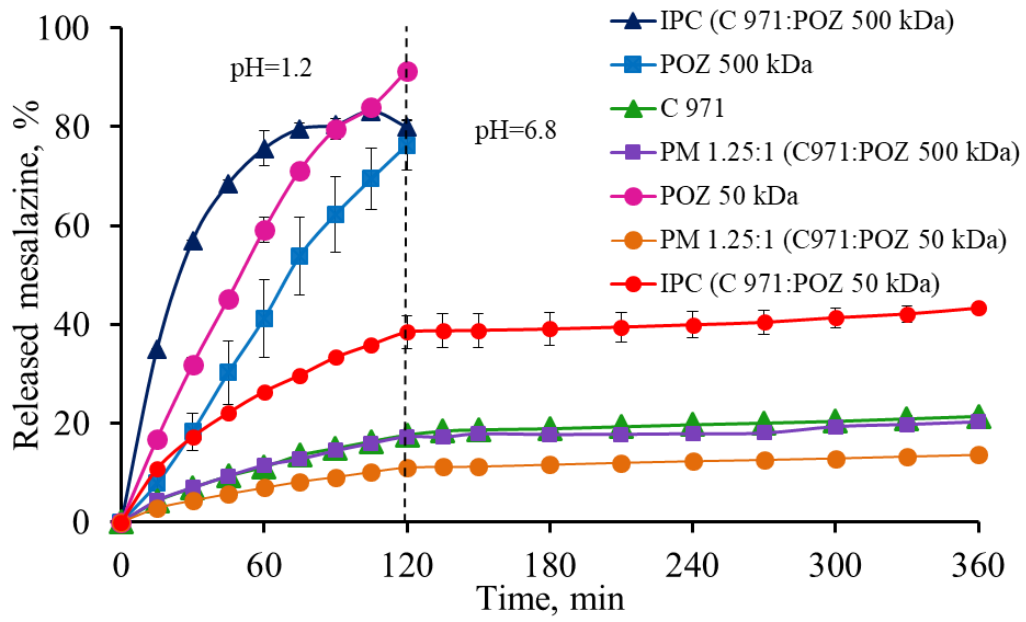


768

769 **Figure 10.** FTIR spectra of IPC based on POZ 50 kDa and C 971 after swelling in the media
 770 mimicking gastro-intestinal tract conditions.

771

772



773

774 **Figure 11.** Release profiles of mesalazine from matrix systems under the conditions mimicking
775 the gastro-intestinal tract.

776